Effects of Dual-Alcohol Gasoline Blends on Physiochemical Properties and Volatility Behavior

Saeid Aghahossein Shirazi[1], Bahareh Abdollahipoor[2], Jake Martinson[1], Bret Windom[2], Thomas D. Foust[2,3], Kenneth F. Reardon[1,3,*]

[1]Department of Chemical and Biological Engineering, Colorado State University, Fort Collins, CO, USA.

[2]Department of Mechanical Engineering, Colorado State University, Fort Collins, CO, USA.

[3]National Renewable Energy Laboratory, Golden, Colorado 80401, USA

Saeid.Aghahossein_Shirazi@colostate.edu

Bahareh.Abdollahipoor@colostate.edu

jmartin664@msn.com

Bret.Windom@colostate.edu

Thomas.Foust@nrel.gov

reardon@colostate.edu

*Corresponding author:

Kenneth F. Reardon

1370 Campus Delivery, Fort Collins, CO, 80523-1370, USA

reardon@colostate.edu

T: +1- 970-491-6505

F: +1-970-491-7369

Abstract

Biofuels can contribute to reducing greenhouse gas emissions from the transportation sector. Ethanol is the main additive for gasoline in the United States, and gasoline containing 10 vol% ethanol is the most commonly used transportation fuel. However, the vapor pressure of these blends is significantly higher than gasoline, which contributes to evaporative emissions. One way to circumvent this and other issues is to use a dual-alcohol approach, mixing lower (methanol or ethanol) and higher alcohols with gasoline to obtain a blend with a vapor pressure close to that of the base gasoline. The goal of this study was to evaluate the fuel potential of dual alcohol blends experimentally and theoretically. Ten dual-alcohol blends were tested at blending ratios from 10 to 80 vol%, with methanol and ethanol used as the lower alcohols and iso-butanol and 3-methyl-3-pentanol as the higher alcohols. The corresponding single alcohol-gasoline blends were also evaluated. For each blend, Reid vapor pressure, vapor lock protection potential, distillation curve, lower heating value, kinematic viscosity, and water tolerance at three temperatures were measured. A model of droplet evaporation was also applied to provide insights into the azeotropic volatility behavior and mixing/sooting potential of the blends. The results of this study show that it is advantageous to use dual-alcohol blends containing up to 40 vol% because they have the characteristics necessary for good performance in existing spark-ignition engines, particularly in terms of volatility, kinematic viscosity, and water tolerance. This study is the first to characterize matched vapor pressure, dual-alcohol blends over a wide blending range as drop-in fuels for conventional spark ignition engines. Furthermore, this was the first investigation of the fuel potential iso-butanol in dual-alcohol blends and of 3-methyl-3-pentanol in single- and dual-alcohol blends.

Keywords: *dual-alcohol, gasoline blend, fuel properties, iso-butanol, 3-methyl-3-pentanol, droplet evaporation, vapor liquid equilibrium, volatility, distillation curve.*

1. Introduction

Overreliance on fossil fuels can lead to serious environmental and price volatility issues. Biofuels have attracted widespread attention due to their capacity to curb the demand for fossil fuels and play a vital role in reducing harmful environmental emissions [1,2]. Among biofuels, bio-alcohols are a promising alternative fuel component for use in spark ignition (SI) engines [3]. In 2011, the U.S. Environmental Protection Agency (EPA) granted a partial waiver for use of fuel blends of up to 15 vol% ethanol in gasoline in passenger cars, light-duty trucks, and flexible-fuel vehicles starting from model year 2001 [4]. In addition, the use of a blend of gasoline and denatured ethanol containing up to 85 vol% ethanol is allowed in flex-fuel vehicles [4].

Alcohols have the potential to replace traditional octane-enhancing strategies minimizing environmental/health impacts while reducing harmful air emissions by closing the carbon cycle and improving energy conversion efficiencies. Conventionally, low molecular weight alcohols such as methanol and ethanol are blended with gasoline. The production processes for these alcohols from renewable sources are well-established, and they are produced at relatively low cost [5]. Blending these alcohols with gasoline enhances the anti-knock properties of the fuel blends and can reduce refinery production costs for high-grade gasoline [6]. The high oxygen content of low molecular weight alcohols results in cleaner combustion, especially with regard to emission of CO and unburned hydrocarbons [5–8]. Low molecular weight alcohols exhibit faster laminar flame speeds than gasoline, which can improve the combustion process [9]. Furthermore, the heat of vaporization (HoV) of these low molecular weight alcohols is significantly higher than that of gasoline, leading to improved thermal efficiencies through the charge cooling phenomenon in both port-fuel and direct-injected SI engines. In addition, charge cooling can help lower peak combustion temperatures, reducing NO_x emissions [10–13].

However, there are limitations to blending low molecular weight alcohols with gasoline. In general, when nonpolar hydrocarbons interact with polar compounds in a mixture, the solution vapor liquid equilibrium can deviate from an ideal solution described by Raoult's law due to the formation of azeotropes. Low molecular weight alcohols such as methanol and ethanol form positive azeotropes with C5−C8 hydrocarbons stemming from the polarity of these molecules [14]. As the polarity of the molecule decreases so does the energy associated with the azeotrope. As such higher alcohols generally exhibit less non-ideal vapor liquid equilibrium than their smaller counterparts. Since positive azeotropes create a mixture which boil at a lower temperature relative to corresponding constituents at their pure states, the vapor pressure of gasoline blends with these alcohols is significantly higher than the base gasoline, contributing to evaporative emissions problems [3]. In addition, low molecular weight alcohols can promote phase separation in the presence of water, especially in cold environments, due to their hygroscopicity and water solubility. This can result in separated alcohol/water mixtures that can be corrosive to the engine and the fuel delivery system [7,15]. Stemming from the large oxygen mass fraction of methanol and ethanol, their lower heating value (LHV) and stoichiometric air-fuel ratios are lower than gasoline. Both factors contribute to increased brake-specific fuel consumption (BSFC), especially if the engine is not tuned to maximize the conversion efficiency for the blended fuel [1,3,7,8,16]. Also, the high HoV of lower alcohols can cause cold start problems under certain operating conditions [17] and can influence the fuel atomization evaporation/mixing phenomenon in direct injection engines, which has implications for particulate matter (PM) formation [18–21].

Considering these limitations, expensive upgrades to existing vehicle architectures and refueling infrastructure are likely to be required to increase the use of low molecular weight alcohols beyond the currently approved 15 vol% [7]. An alternative approach to increasing the fraction of biofuel in a gasoline blend is to co-blend higher alcohols (any saturated mono-alcohol with three

or more carbon atoms). Higher alcohols are effective options for blending with lower alcohols in gasoline because (1) higher alcohols can be produced from renewable feedstocks through either fermentation or catalytic conversion of syngas, although the cost of production is currently higher than lower alcohols [22]; (2) they are less corrosive to materials in the fuel delivery and injection systems compared to lower alcohols [1]; (3) higher alcohols can increase the water tolerance of alcohol-gasoline blends, especially compared to methanol blends with gasoline [23,24]; (4) they exhibit better lubrication and contribute to less engine wear as a result of their higher viscosity [7]; (5) they have a higher lower heating value (LHV) than lower alcohols as a result of decreased oxygen mass fraction, resulting in better fuel economy [8]; and (6) their lower vapor pressures and reduced azeotropic activity can mitigate many of the evaporation-driven concerns associated with lower alcohols [25].

Andersen et al. [26] described the concept of mixing a lower alcohol and a higher alcohol (ethanol and 1-butanol) in gasoline to obtain an alcohol-gasoline blend with a Reid vapor pressure (RVP) matching that of the base gasoline. Only a few studies have been conducted to test dual-alcohol blends using this approach. Siwale et al. [27]compared M70 (methanol 70 vol% + gasoline 30 vol%) with a blend containing 53 vol% methanol, 17 vol% n-butanol and 30 vol% gasoline. Compared to M70, the dual-alcohol blend provided shortened combustion duration, better volumetric efficiency, higher energy content, and better brake thermal efficiency, while the RVP remained the same as that of gasoline. Ratcliff et al. [28] compared the effects on light-duty vehicle exhaust emissions of four blends with 5.5 wt% oxygen: a dual-alcohol blend (12 vol% iso-butanol + 7 vol% ethanol) and three single-alcohol gasoline blends (16 vol% ethanol, 17 vol% n-butanol, and 21 vol% iso-butanol). The emissions of the dual-alcohol blend had the lowest levels of NO_x, non-methane organic gas, and unburned alcohols.

These reports suggest that dual-alcohol blends can be advantageous. However, there has not yet been a characterization of matched-RVP, dual-alcohol blends over a wide blending volume range to examine their potential as drop-in fuel for conventional spark ignition engines. The goal of this study was to characterize important physiochemical properties of dual-alcohol gasoline blends and to assess how these blends are compatible with the current standard specification for automotive spark ignition engine fuel (ASTM D4814). Properties of dual-alcohol blends were also compared to the base gasoline and corresponding single-alcohol blends. The two higher alcohols used in the dual-alcohol blends were iso-butanol and 3-methyl-3-pentanol (3M3P), identified as promising higher alcohols for blending with gasoline in our previous study [29]. In addition to fuel property determination, an advanced distillation apparatus was used to obtain distillation curves and distillate composition for all blends. A distillation-based droplet evaporation model validated with the experimental data was used to provide insights on volatility differences and the in-cylinder mixing potential between the dual-alcohol blends, single alcohol blends, and gasoline.

2. Materials and Methods

2.1. Test fuels

The base gasoline used was an unleaded test gasoline (UTG-96) from Phillips 66. The measured RVP of this gasoline was 52 kPa. Methanol (99.9%, Certified ACS) and ethanol (200 proof) were obtained from Fisher Scientific. Iso-butanol (≥ 99 %, FG) and 3-methyl-3-pentanol (≥ 99 %, FG) were obtained from Sigma-Aldrich. A total of 25 gasoline alcohol blends as well as the neat gasoline were tested in this study. Total alcohol blending volumes spanning from 10–80 vol% were considered to investigate the effect of increased alcohol usage on the fuel specifications.

Dual-alcohol blends were selected to control RVP with the intent to reduce the issues associated with the increased volatility of single alcohol-gasoline blends. The concentration of lower and higher alcohols in each dual-alcohol blend was obtained by using the equation proposed by Anderson et al. [26] aiming to match the RVP of the blend with that of the base gasoline:

$$C_i = \left(\frac{RVP_G - RVP_j(@C_t)}{RVP_i(@C_t) - RVP_j(@C_t)}\right) \times C_t \quad \text{Eq. 1}$$

Here, C_i is the volume fraction of alcohol i, C_t is the total alcohol volume fraction, RVP_G is the RVP of the base gasoline, and $RVP_i(@C_t)$ and $RVP_j(@C_t)$ are RVPs of the single alcohol gasoline blends i and j each at a blending ratio of C_t, respectively. Volumetric concentrations of lower and higher alcohols for each dual-alcohol blend are presented in Table 1. In this work, G, M, E, B, and H represent gasoline, methanol, ethanol, iso-butanol, and 3M3P, respectively. Since 3M3P is a hexanol isomer, it is represented by the letter "H". Each blend is abbreviated with an alphanumeric code in which the letter (or letters) represents the alcohol (or alcohols) used in the blend and the number represents the total alcohol volume fraction. For instance, H10 consists of 10 vol% 3M3P and 90 vol% gasoline while MB80 consists of 80 vol% total alcohol (74 vol% methanol + 6 vol% iso-butanol) and 20 vol% gasoline.

In general, ethanol is a superior fuel to methanol due to its lower RVP, lower corrosivity, better water tolerance, and higher heating value [7]. Therefore, ethanol was used to make dual-alcohol blends for blending ratios of 10, 20 and 40 vol%. However, since the RVPs of E60 and E80 are less than the RVP of the base gasoline, it is not possible to make matched-RVP dual-alcohol blends with ethanol at those higher levels. Thus, methanol was used for the higher blending

177 ratios (60 and 80 vol%). Comparison of the dual-alcohol blends containing 60 vol% or more total
178 alcohol were compared to corresponding methanol (single-alcohol) blends.
179
180

Table 1. List of test blends. M: methanol. E: ethanol. B: iso-butanol. H: 3-methyl-3-pentanol.

Total alcohol volume fraction (vol%)	Methanol blends	Ethanol blends	iso-Butanol blends	3M3P blends	Dual-alcohol blends containing iso-butanol (lower alcohol vol%+ iso-butanol vol%)	Dual-alcohol blends containing 3M3P (lower alcohol vol%+3M3P vol%)
10	–	E10	B10	H10	EB10 (2.7 vol% E +7.3 vol% B)	EH10 (3.3 vol% E + 6.7 vol% H)
20	–	E20	B20	H20	EB20 (8.9 vol% E +11.1 vol% B)	EH20 (11.5 vol% E + 8.5 vol% H)
40	–	E40	B40	H40	EB40 (33.1 vol% E +6.9 vol% B)	EH40 (36.3 vol% E + 3.7 vol% H)
60	M60	–	B60	H60	MB60 (34.5 vol% M +25.5 vol% B)	MH60 (37.8 vol% M + 22.2 vol% H)
80	M80	–	B80	H80	MB80 (74 vol% M + 6 vol% B)	MH80 (75 vol% M + 5 vol% H)

2.2. Methods

The test fuel blends were prepared and kept in a freezer to minimize evaporative losses. The RVP, vapor lock protection potential, temperature dependent water tolerance, LHV, density, and viscosity were characterized for each fuel. These properties were measured three times for each sample. RVP and vapor lock protection potential were measured using the Grabner Instruments Minivap VPXpert vapor pressure analyzer according to ASTM 5191 [30] and ASTM D5188 [31], respectively. RVP was measured for single alcohol-gasoline blends at 1, 2, 3, 5, 10, 15, 20, 30, …, 90, and 100 vol%. For dual-alcohol blends, RVP was measured at 10, 20, 40, 60, and 80 vol% total alcohol. Water tolerance was measured at three target temperatures, +10, 0, and –10 °C, by gradually adding water to the tempered blend until phase separation was observed. The water tolerance was defined as the percent volume of water added over the total volume of the blend. The LHV was measured with an IKA C200 calorimeter according to ASTM D240-14 [32]. An Anton-Paar SVM 3000 viscometer-densitometer was used to measure viscosity and density.

A custom-built Advanced Distillation Curve (ADC) apparatus was employed to conduct the distillation curve measurements at 84.3 kPa. The ADC apparatus and method are comprehensively described elsewhere [33]. The distillation was conducted twice for each sample. Moreover, to scrutinize the effect of replacing a portion of ethanol with a higher alcohol on the composition evolution during the distillation, samples were acquired at the first drop, 10, 20, 30, 40, 50, 60, 70, 80, and 90 vol% distilled for the most promising dual-alcohol blends (10, 20 and 40 vol%) in addition to corresponding ethanol blends and gasoline for comparison. The sampled distillate composition was quantified according to ASTM D6729 [34] using an HP 5890 Series II GC-FID equipped with 100-m long Petrocol DH fused-silica capillary column coated with polydimethyl siloxane. Chromatogram peak areas were converted to the mass concentrations following calibration. Average molecular weight was calculated using the mass fraction and the molecular weight of each component.

2.3 Droplet evaporation model

In this study, the droplet evaporation model developed by Burke et al. [35] was used to simulate the evaporation of fuel droplets to obtain thermodynamically driven evaporation times. The evaporation time can be used to estimate differences in mixing time scales between two fuel mixtures and the potential of the blends to form PM [36]. This model uses the same algorithm as distillation model developed by Backhaus [37], but to model the distillation of the fuels as droplets, the D^2 law and appropriate energy and mass conservation equations are incorporated. In these models, the UNIFAC group contribution was utilized to take the non-ideality into account. The complex fuel was simulated using 54 components. The list of the simplified composition for gasoline UTG-96 is presented in Table S1. Using the simplified composition, a mass fraction weighted average approach described by Chupka et al. [38] was used to determine transient HoV and droplet evaporation time.

3. Results and discussion

3.1. Volatility

3.1.1. Reid vapor pressure

The RVPs of all tested alcohols and blends with gasoline are shown in Tables 2 and 3 and Figure 1. Since the desirable volatility of a SI engine fuel is different for each season and location, ASTM D4814 specifies six vapor pressure/distillation and vapor lock protection classes, as shown in Table S2.

Table 2. Properties of pure alcohols. Values are shown as the mean +/- one standard deviation of triplicate measurements. BP: normal boiling point; ρ: density @ 20 °C; μ: dynamic viscosity @ 20°C; v: kinematic viscosity @ 20 °C. [a] Obtained from [29]. [b] Obtained from [39].

Alcohol	RVP (kPa)	BP (°C) [a]	HoV at 25 °C (kJ/kg) [b]	LHV (kJ/g)	ρ (g/cm^3)	μ (cP)	v (mm^2/s)
Methanol	30.75 ± 0.35	64.70	1169.3	22.43 ± 0.28	0.79 ± 0.0	0.55 ± 0.1	0.70 ± 0.1
Ethanol	14.88 ± 0.41	78.20	924.1	28.89 ± 0.31	0.79 ± 0.0	1.18 ± 0.2	1.50 ± 0.2
Iso-butanol	2.09 ± 0.02	107.80	701.9	36.40 ± 0.38	0.80 ± 0.0	4.06 ± 0.1	5.07 ± 0.1
3-methyl-3-pentanol	1.12 ± 0.29	122.40	474.0	38.39 ± 0.04	0.83 ± 0.0	5.43 ± 0.3	6.56 ± 0.3

Table 3. Measured properties of tested fuels. Error ranges correspond to +/- one standard deviation of duplicate measurements for distillation temperatures and triplicate measurements for the other tests. RVP: Reid vapor pressure. IBP: Initial boiling point. EP: end-point. ρ: Density @ 20 °C. μ: Dynamic viscosity @ 20°C. ν: Kinematic viscosity @ 20 °C. WT: water tolerance (vol %). M: methanol. E: ethanol. B: iso-butanol. H: 3-methyl-3-pentanol.

Fuel	RVP (kPa)	$T_{v/l=20}$ (°C)	IBP (°C)	T10 (°C)	T50 (°C)	T90 (°C)	LHV (kJ/g)	ρ (g/cm^3)	μ (cP)	ν (mm^2/s)	WT (vol%)		
											+10 °C	0 °C	−10 °C
Gasoline	52.07 ± 0.83	65.96 ± 0.66	52 ± 0	73 ± 0	105 ± 0	153 ± 5	45.72 ± 0.20	0.74 ± 0.0	0.37 ± 0.03	0.50 ± 0.03	0 ± 0	0 ± 0	0 ± 0
E10	59.63 ± 0.25	56.63 ± 0.17	49 ± 1	61 ± 0	103 ± 0	142 ± 2	43.95 ± 0.60	0.74 ± 0.0	0.39 ± 0.01	0.53 ± 0.01	0.3 ± 0.0	0.2 ± 0.0	0.2 ± 0.0
B10	50.75 ± 0.09	66.53 ± 0.31	56± 2	75 ± 1	100 ± 2	144 ± 13	44.60 ± 0.22	0.77 ± 0.0	0.55 ± 0.01	0.71 ± 0.01	0 ± 0	0 ± 0	0 ± 0
H10	49.95 ± 0.09	69.00 ± 0.86	56 ± 1	78 ± 1	106 ± 1	146 ± 6	44.76 ± 0.11	0.75 ± 0.0	0.43 ± 0.01	0.58 ± 0.02	0 ± 0	0 ± 0	0 ± 0
EB10	53.44 ± 0.09	62.17 ± 0.24	51 ± 1	71 ± 0	101 ± 1	143 ± 1	44.44 ± 0.15	0.75 ± 0.0	0.44 ± 0.04	0.58 ± 0.05	0 ± 0	0 ± 0	0 ± 0
EH10	55.89 ± 0.07	61.57 ± 0.42	48 ± 1	66 ± 1	103 ± 1	144 ± 1	44.39 ± 0.05	0.75 ± 0.0	0.44 ± 0.01	0.59 ± 0.02	0 ± 0	0.0 ± 0.0	0.0 ± 0.0
E20	58.21 ± 0.41	57.20 ± 0.00	47 ± 0	60 ± 0	74 ± 0	144 ± 3	42.46 ± 0.13	0.75 ± 0.0	0.47 ± 0.01	0.62 ± 0.01	0.7 ± 0.0	0.6 ± 0.0	0.5 ± 0.0
B20	48.47 ± 0.20	67.83 ± 0.46	54 ± 0	74 ± 1	96± 0	135 ± 4	43.73 ± 0.43	0.75 ± 0.0	0.53 ± 0.01	0.70 ± 0.01	0.0 ± 0.0	0.0 ± 0.0	0.0 ± 0.0
H20	46.59 ± 0.45	70.73 ± 0.24	56± 0	82 ± 1	108 ± 1	138 ± 2	44.34 ± 0.35	0.75 ± 0.0	0.50 ± 0.01	0.67 ± 0.02	0 ± 0	0 ± 0	0 ± 0
EB20	53.17 ± 0.16	62.03 ± 0.59	50 ± 1	65 ± 0	89 ± 0	134 ± 1	42.68 ± 0.42	0.75 ± 0.0	0.51 ± 0.00	0.68 ± 0.00	0.0 ± 0.0	0.0 ± 0.0	0.0 ± 0.0
EH20	54.96 ± 0.18	60.30 ± 0.51	49 ± 1	63 ± 1	94 ± 1	137 ± 01	42.93 ± 0.45	0.75 ± 0.0	0.48 ± 0.01	0.64 ± 0.02	0.6 ± 0.0	0.5 ± 0.0	0.4 ± 0.0

E40	53.97 ± 0.13	60.07 ± 0.17	50 ± 1	62 ± 1	73 ± 1	140 ± 1	38.83 ± 0.37	0.77 ± 0.0	0.67 ± 0.01	0.88 ± 0.01	2.6 ± 0.0	2.3 ± 0.0	2.1 ± 0.0
B40	41.52 ± 0.16	74.57 ± 0.39	55 ± 0	79 ± 1	97 ± 1	110 ± 2	41.71 ± 0.45	0.77 ± 0.0	0.83 ± 0.01	1.09 ± 0.01	0.2 ± 0.0	0.1 ± 0.0	0.0 ± 0.0
H40	39.64 ± 0.10	78.63 ± 0.69	62 ± 0	91 ± 0	112 ± 0	128 ± 0	42.64 ± 0.64	0.77 ± 0.0	0.74 ± 0.01	0.95 ± 0.01	0.0 ± 0.0	0.0 ± 0.0	0.0 ± 0.0
EB40	51.98 ± 0.04	61.20 ± 0.22	50 ± 0	65 ± 0	76 ± 0	108 ± 0	39.00 ± 0.39	0.77 ± 0.0	0.72 ± 0.01	0.94 ± 0.01	3.2 ± 0.0	3 ± 0.0	2.6 ± 0.0
EH40	53.61 ± 0.15	60.23 ± 0.26	48 ± 1	63 ± 1	74 ± 1	126 ± 1	39.43 ± 0.06	0.76 ± 0.0	0.65 ± 0.01	0.85 ± 0.01	3.0 ± 0.0	2.7 ± 0.0	2.4 ± 0.0
M60	67.1 ± 0.53	51.53 ± 0.21	44 ± 0	54 ± 1	60 ± 1	62 ± 1	30.52 ± 0.35	0.77 ± 0.0	0.53 ± 0.04	0.69 ± 0.05	0.6 ± 0.0	0.3 ± 0.0	0.1 ± 0.0
B60	32.5 ± 0.35	83.07 ± 0.29	69 ± 0	88 ± 1	101 ± 0	106 ± 0	39.13 ± 0.41	0.78 ± 0.0	1.50 ± 0.01	1.92 ± 0.01	2.4 ± 0.0	1.8 ± 0.0	1.6 ± 0.0
H60	28.59 ± 0.16	86.57 ± 0.90	74 ± 2	102 ± 0	116 ± 1	124 ± 0	41.29 ± 0.08	0.79 ± 0.0	1.22 ± 0.01	1.54 ± 0.01	0.0 ± 0.0	0.0 ± 0.0	0.0± 0.0
MB60	56.65 ± 0.20	56.47 ± 0.12	49 ± 0	60 ± 0	72 ± 0	106 ± 0	33.96 ± 0.17	0.77 ± 0.0	0.75 ± 0.05	0.97 ± 0.07	4.4 ± 0.0	4 ± 0.0	3.5 ± 0.0
MH60	58.10 ± 0.17	55.80 ± 0.16	46 ± 0	58 ± 1	69 ± 1	124 ± 1	34.25 ± 1.22	0.78 ± 0.0	0.78 ± 0.03	1.00 ± 0.03	4.2 ± 0.0	3.8 ± 0.0	3.4 ± 0.0
M80	54.73 ± 0.15	56.63 ± 0.05	49 ± 0	58 ± 0	61 ± 0	62 ± 1	25.73 ± 0.98	0.78 ± 0.0	0.55 ± 0.01	0.70 ± 0.01	3.1 ± 0.0	2.7 ± 0.0	2.2 ± 0.0
B80	19.56 ± 0.43	89.50 ± 0.00	83 ± 1	99 ± 0	105 ± 0	107 ± 0	36.62 ± 1.08	0.79 ± 0.0	2.38 ± 0.01	3.02 ± 0.01	3.5 ± 0.0	2.9 ± 0.0	2.7 ± 0.0
H80	15.74 ± 0.70	86.47 ± 1.23	91 ± 0	111 ± 0	118 ± 0	122 ± 1	39.84 ± 0.23	0.81 ± 0.0	2.23 ± 0.02	2.76 ± 0.03	0.0 ± 0.0	0.0 ± 0.0	0.0 ± 0.0
MB80	54.18 ± 0.13	56.93 ± 0.09	50 ± 1	59 ± 0	63 ± 0	72 ± 3	27.61 ± 0.06	0.78 ± 0.0	0.57 ± 0.02	0.73 ± 0.02	3.5 ± 0.0	2.9 ± 0.0	2.2 ± 0.0
MH80	52.59 ± 1.70	56.73 ± 0.12	51 ± 1	60 ± 1	63± 1	117 ± 1	27.67 ± 0.10	0.78 ± 0.0	0.58 ± 0.02	0.74 ± 0.02	4 ± 0.0	3.4 ± 0.0	2.9 ± 0.0

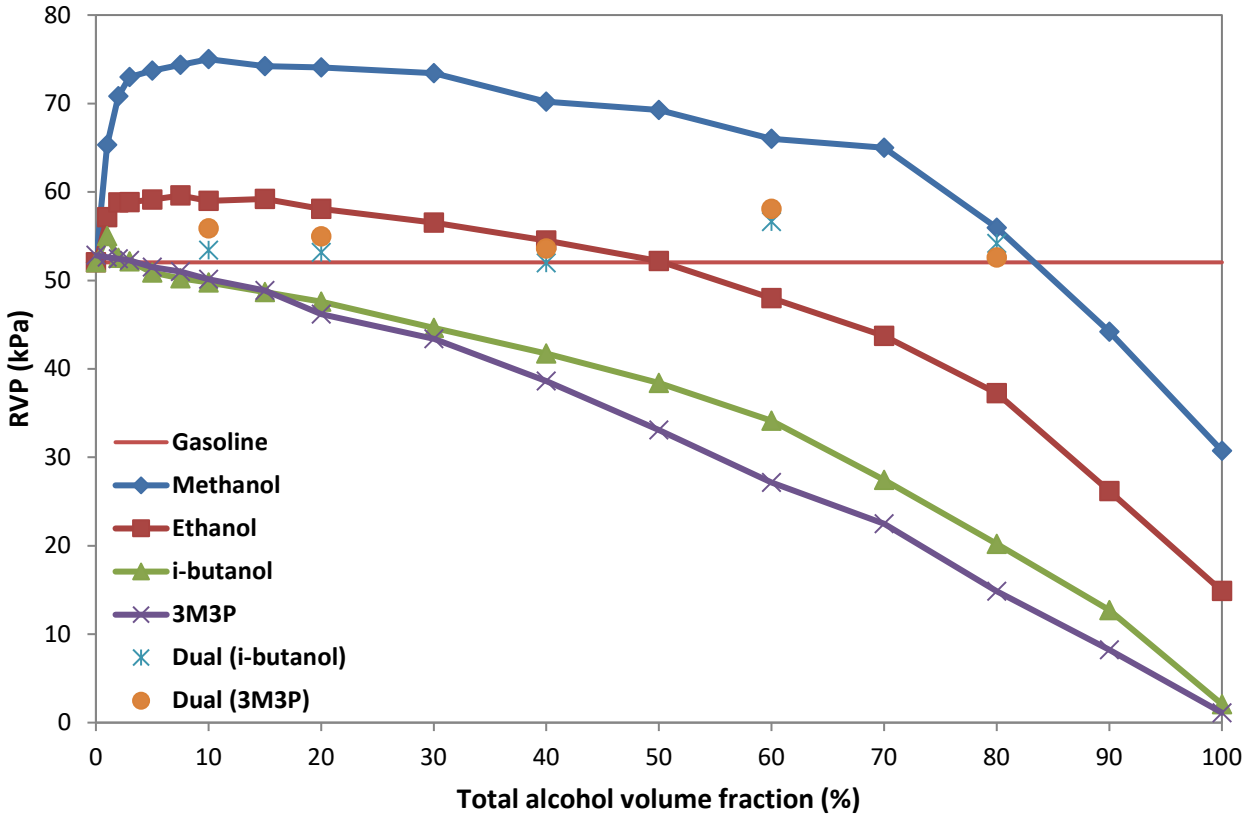

Figure 1. The relationship between RVP and total fraction of alcohol for each test fuel. Points are the average of triplicate measurements. The average standard error for all data points is 0.3 kPa.

The RVP of methanol and ethanol gasoline blends are highly affected by non-ideal vapor-liquid equilibrium mixture behavior (Figure 1). While the RVPs of pure methanol and ethanol are lower than that of the gasoline, the formation of positive azeotropes in the mixture of lower alcohols and gasoline results in higher vapor pressures than the gasoline below 80 vol% methanol and 50 vol% ethanol. The highest RVP (74.2 kPa) was observed for a blend containing 10 vol% methanol. Among the ethanol blends, the highest RVP was observed for E15 (59.2 kPa). All

blends with only methanol and ethanol qualified under ASTM D4814, although in different volatility classes: Class AA for blends containing more than 50 and 80 vol% ethanol and methanol; Class A for ethanol blends with less than 50 vol% ethanol; Class C for methanol blends with less than 50 vol% methanol; and Class B for methanol blends containing 50 to 80 vol% methanol.

There is a clear trend of decreasing RVP with the increase in alcohol concentration for the blends containing only a higher alcohol (i.e., iso-butanol and 3M3P) except for the blend containing 1 vol% of iso-butanol (Figure 1). This confirms that as the carbon number is increased, the azeotropic effect of hydroxyl group is dissipated such that the higher alcohol blends behave as ideal mixtures. All the blends containing a single higher alcohol qualified under ASTM D4814 for all classes due to their low RVP values, especially at high blending ratios. Since gasoline is very volatile, lowering the RVP of gasoline to a certain point is generally desired because it is expensive to produce a low RVP gasoline [40]. Therefore, the use of higher alcohols can be advantageous. However, cold starting requires a minimum vapor pressure especially when considering high HoV fuels containing alcohols. Although no minimum limit is specified in the ASTM D4814 for vapor pressure, the low RVPs of blends containing a high concentration of higher alcohols are not desirable because it may cause cold start problems.

The dual-alcohol blends were designed to have an RVP that matched that of gasoline, and this was confirmed by measurement: all dual-alcohol blends had an RVP within 9% of that of the base gasoline (Table 3). A small number of the measured values were slightly higher than the target gasoline RVP, which may be due to non-linear blending effects that are not accounted for in Eqn. 1. Nevertheless, Eq. 1 proved to be a good predictor of RVP for the dual-alcohol blended fuels.

3.1.2. Vapor lock protection potential

The best index to assess hot fuel handling problems is vapor lock protection potential ($T_{V/L=20}$), which is the temperature at which a fuel forms a volumetric vapor-liquid ratio of 20 at atmospheric pressure. Six vapor lock protection classes for minimum $T_{V/L=20}$ are specified in ASTM D4814. All tested blends met ASTM specifications for all volatility classes except M60 with a $T_{V/L=20}$ of 51.53 °C, which qualifies for all classes other than Class 1 (min $T_{V/L=20}$ of 54). Blends containing high concentration of single higher alcohols (60 and 80 vol%) had the highest (i.e., were the least likely to exhibit vapor lock) $T_{V/L=20}$ due to their very low volatility. The M60 blend had the lowest vapor lock index, followed by the low fraction ethanol blends (E10 and E20) because of the azeotrope-driven volatility of these blends. Dual-alcohol blends containing up to 40 vol% of total alcohol successfully maintained vapor lock indices close to that of gasoline. The $T_{V/L=20}$ of the dual-alcohol blends with higher blending ratios (60 and 80 vol%) was reduced due to their high concentration of methanol but those values were still high enough to meet all ASTM class requirements.

3.1.3. Distillation curve

ASTM D4814 sets acceptable boundaries for distillation temperatures for fuels used in SI engines. To ensure that a fuel provides an appropriate volatility, this standard specifies maximum limits on T10, T50, T90, and end-point and minimum limits for T50 for six distillation classes. Distillation curves are available in Figures S1 to S5 for each total initial alcohol content fuel. Distillation temperatures at 84.3 kPa (initial boiling point, T10, T50, and T90) for each blend are listed in Table 3. The distillation curve of the unblended gasoline is smooth and steadily increasing. The addition of lower alcohols (methanol and ethanol) to gasoline increased the volatility through the formation of positive azeotropes and caused a reduction in the front-end (T0-T20) and mid-range (T20-T90) distillation temperatures. For the blends with individual lower

alcohols, once the alcohol evaporated, a relatively sharp rise in boiling temperatures was observed as the distillation approached the boiling temperatures of the gasoline components. This behavior was observed in low to medium (10 to 40 vol%) blending ratios. For higher blending ratios, the suppressed boiling temperature behavior existed throughout the entirety of the measured distillation, resulting in nearly isothermal boiling temperatures. The end-point temperature decreased in the alcohol blends due to the dilution of heavy hydrocarbons.

In contrast to the lower alcohols, the blends with higher alcohols exhibited little to no azeotropic behavior. In the early stages, the distillation curves of these blends are above the distillation curve of the base gasoline due to the high boiling points and low RVPs of the added alcohol. Once the alcohol was evaporated, the trend of the distillation temperatures became similar to that of the gasoline. As the concentration of the higher alcohol in the blend increases, the point at which the distillation temperatures approach that of the gasoline occurs at higher distilled volume fractions. The temperatures at the tail end of the distillation curve for the high alcohol fuel blends are lower than those of gasoline due to dilution of the heavy hydrocarbon fraction. In all blending ratios, 3M3P reduced the volatility of the gasoline more so than iso-butanol owing to its higher boiling point, lower RVP, and lower polarity.

Distillation curves for the dual-alcohol blends are between the curves of the corresponding single-alcohol blends. At the beginning of the distillation, temperatures were closer to those of the corresponding individual lower alcohol blend while at higher volume fractions, once most of the lower alcohol was evaporated, there was a sharp rise in boiling temperatures as the distillation curve converged to that of the blend containing a single higher alcohol. The blends containing methanol and 3M3P (MH60 and MH80) provided the clearest example of this trend as these blends were comprised of the alcohol combination with the widest range in RVP, and the most and least polar alcohols used in this study.

The distillation temperatures were also compared to the ASTM D4814 limits to investigate the compatibility of these blends with the current standards. In this study, distillation curves were obtained at 84.3 kPa, while ASTM D8418 sets limits at 1 atm. Therefore, temperature measurements were corrected to 101.3 kPa using the Sydney-Young equation as stated in ASTM D86 [41]. Corrected distillation temperatures for 1 atm are available in Table S3.

The maximum limit in ASTM D4814 for T10 is 70 °C for Class AA, while its value is 50 °C for Class E (Table S2). The T10 for the gasoline used in this study was 77.9 °C, which is not within the acceptable range. GC-FID analysis of the gasoline revealed high concentrations of heavy olefins and aromatics. The relatively low RVP and high molecular weight of these compounds led to the high T10 for the gasoline. Therefore, none of the higher alcohol blends passed the T10 requirements with this low-volatile gasoline because they tend to increase the T10 of the fuel. All blends with single lower alcohols as well as some dual-alcohol blends (EH20, EG40, MB60, MH60, MB80, and MH80) have T10 values that meet ASTM D4814 class specifications.

The ASTM D4814 allowable minimum T50 value is 77 °C for all classes. The ASTM D4814 maximum for T50 varies from 110 °C for Class E to 120 °C for Class AA. Five blends, each containing methanol, do not meet the minimum T50 (M60, M80, MH60, MB80, and MH80). Two 3M3P blends exceeded the maximum T50 requirement (H60 and H80) because of the high boiling temperature of 3M3P.

The tail-end volatilities (T90-end point) for all blends are below that of gasoline, all passing the T90 maximum requirement. Considering all these limitations together, using this gasoline, which was not qualified itself due to the high T10, only six blends (E10, E20, EH20, E40, EH40, MB60)

qualified for distillation curve Class AA. A list of the blends qualified for each distillation class for each distillation temperature is tabulated in Table 4.

Table 4. Blends that are qualified for each distillation class for each distillation temperature

	Qualified blends at the indicated distillation temperatures		
Distillation classes	**T10**	**T50**	**T90**
AA	E10, E20, EH20, E40, EH40, MB60	Gasoline, E10, B10, H10, EB10, EH10, E20, B20, H20, EB20, EH20, E40, B40, H40, EB40, EH40, B60, B80	All the test fuels
A	E10, E20, EH20, E40, EH40, MB60	Gasoline, E10, B10, H10, EB10, EH10, E20, B20, H20, EB20, EH20, E40, B40, H40, EB40, EH40, B60, B80	All the test fuels
B	–	Gasoline, E10, B10, H10, EB10, EH10, E20, B20, H20, EB20, EH20, E40, B40, H40, EB40, EH40, B60, B80	All the test fuels
C	–	Gasoline, E10, B10, H10, EB10, EH10, E20, B20, H20, EB20, EH20, E40, B40, H40, EB40, EH40, B60, B80	All the test fuels
D	–	Gasoline, E10, B10, H10, EB10, EH10, E20, B20, EB20, EH20, E40, B40, EB40, EH40, B60, B80	All the test fuels
E	–	E10, B10, EB10, EH10, E20, B20, EB20, EH20, E40, B40, EB40, EH40, B60	All the test fuels

3.1.4. Distillate Composition

The presence of alcohol(s), in particular ethanol, suppressed the distillation of aromatic species, as is apparent from the sharp rise in aromatic concentration once ethanol was evaporated (Figure 2). This sharp rise occurred later during the distillation for the blends containing higher

concentrations of ethanol. This aromatic enrichment occurred because ethanol evaporated early, delaying the evaporation of the heavier aromatics. Previous work has shown that azeotropes formed with ethanol can play a minor role in the observed aromatic enrichment [36]. In most of the blends containing only ethanol, the mass fraction of aromatics at the late stages of the distillation (e.g., 90 vol%) are very similar to the neat gasoline despite having a much lower total fraction of aromatics than the base gasoline due to dilution. Comparing the dual-alcohol blends with the ethanol-only blends, the dual-alcohol blends (especially those with 3M3P) resulted in 4.2-30.3% lower aromatic concentrations compared to gasoline at the 90 vol% distilled point, indicating that that the aromatics were in the remaining fuel. Since aromatics generally have shorter kinetic pathways to soot compared to other types of hydrocarbons present in gasoline [33], there is an increased susceptibility of PM formation when aromatics make up the heavy fraction of the fuel. Thus, oxygenated blends, especially dual-alcohol blends, may lead to an increase in PM emissions. It is worth noting that it is only one of many parameters that can affect the level of PM emissions. Other factors, including engine parameters, test conditions, fuel spray break-up, and air mixing, could potential modulate the formation of PM in oxygenated blends.

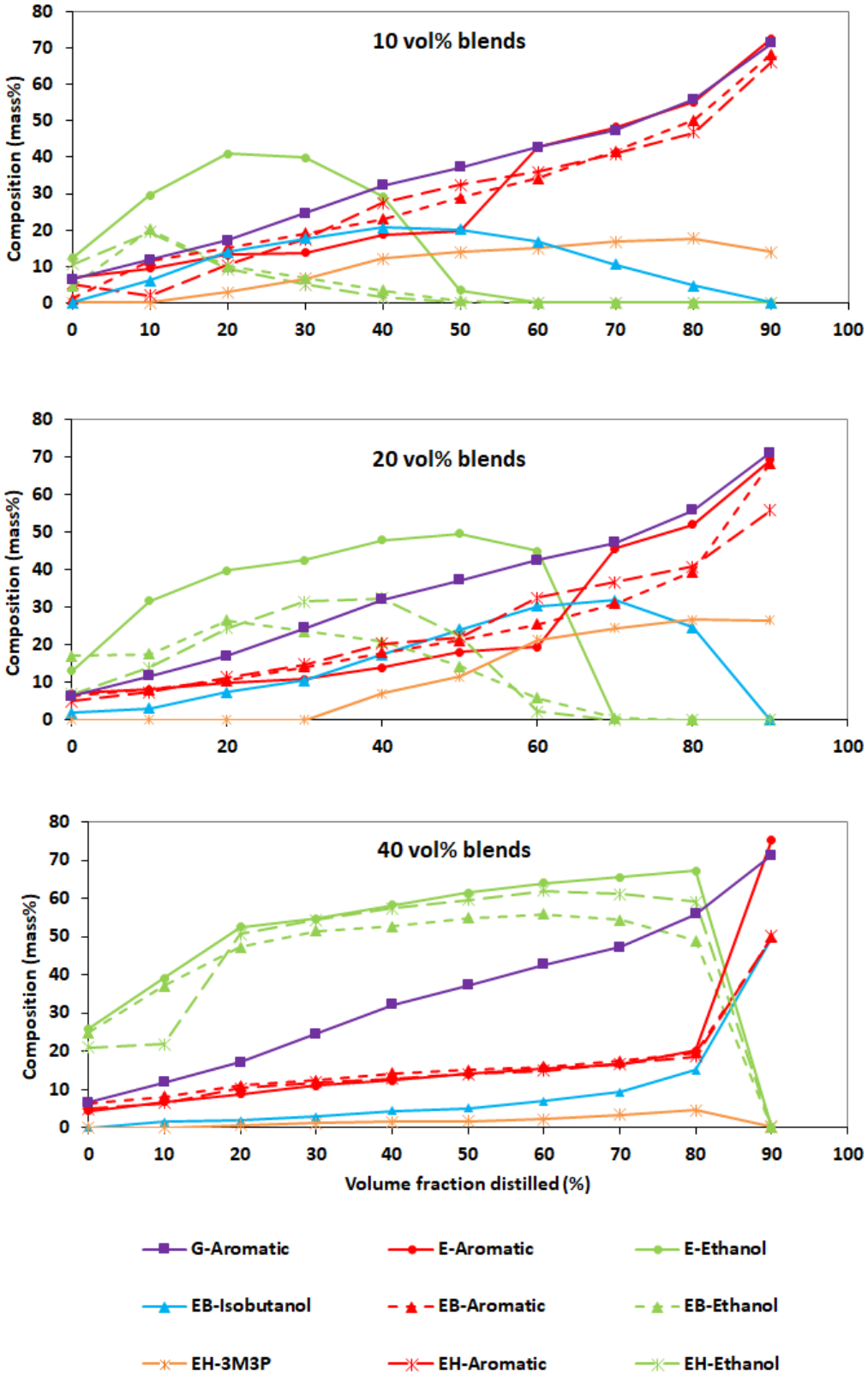

Figure 2. Distillate composition analysis for gasolines and blends containing up to 40% alcohol. The average coefficient of variation of all data points is 2.5% for aromatics and 3.7% for oxygenates from duplicate distillation tests. G-Aromatic: Mass percent of aromatics in gasoline. E-Aromatic: Mass percent of aromatics in ethanol blends. EB-Aromatic: Mass percent of aromatics in dual-alcohol blends containing iso-butanol. EH-Aromatic: Mass percent of aromatics in dual-alcohol blends containing 3M3P. E-Ethanol: Mass percent of ethanol in ethanol blends. EB-Ethanol: Mass percent of aromatics in dual-alcohol blends containing iso-butanol. EH-Ethanol: Mass percent of aromatics in dual-alcohol blends containing 3M3P. EB-Iso-butanol: Mass percent of iso-butanol in dual-alcohol blends containing iso-butanol. EH-3M3P: Mass percent of 3M3P in dual-alcohol blends containing 3M3P.

3.1.5. Distillation model validation

The distillation model accurately predicted the temperature inflection points for each of the mixtures and the corresponding composition changes, as seen in comparisons of distillation curves and molecular weight (Figures S6-S11). The overall agreement validates the accuracy of the distillation model and its use to predict droplet evaporation [35].

3.1.6. Droplet lifetime

Many parameters such as the injector nozzle design, operational conditions, and physical properties of a fuel can influence spray atomization and droplet size distributions. In particular, density, viscosity, and surface tension are known to be important factors that describe the atomization of a liquid fuel. The specific gravity of the gasoline increased with the addition of alcohols, especially with higher alcohols (Table 3). The densities of the dual-alcohol blends were between the density of corresponding higher and lower alcohol blends. The kinematic viscosity increased with increase in alcohol content (Figure 3). The kinematic viscosity for the

individual higher alcohol blends (iso-butanol and 3M3P) increased more rapidly and in a non-linear fashion compared to the blends containing only a single lower alcohol. The dual-alcohol blends exhibited viscosities closer to that of gasoline. Fuels with higher density and viscosity form larger droplet sizes, which can cause poor fuel atomization and may result in a heterogeneous mixture and accordingly more susceptibility to higher PM emissions [42]. The surface tensions of the blends were predicted by the DIPPR database [39] and the values for all blends were very close to the value for gasoline. The model developed by Elktob [43] is a semi-empirical correlation which considers the critical fuel properties (viscosity, surface tension and density) and nozzle conditions to estimate spray characteristics with high accuracy as seen in [44]. Thus, this model was exploited to determine the droplet size of all the fuel blends (relative to that of gasoline) and show how the addition of alcohol components with varying molecular weight/concentrations impact the spray atomization process and droplet sizes.

$$\text{Sauter Mean Diameter} = 3.085 v_l^{0.385} \sigma_l^{0.737} \rho_l^{0.737} \rho_g^{0.06} \Delta P_l^{-0.54} \quad \text{Eq. 2}$$

In Eqn. 2, v_l is the viscosity of liquid, ρ_l and ρ_l are the gas and liquid density, σ_l is the surface tension of liquid, and ΔP_l *is* the difference between injection pressure and ambient pressure. For an initial droplet diameter of gasoline of 25 μm, which is in the usual range for mean droplet diameters observed in traditional DISI injector technology [45], and maintaining the same ΔP_l for all blends, the initial droplet sizes of all other blends were determined relative to that of gasoline with Eq. 2 and the physical properties listed in Table 5. The droplet evaporation model was then used with the calculated droplet sizes for each blend at constant ambient temperature (323 K) and standard atmospheric pressure to determine the influence of droplet size on droplet evaporation lifetimes.

In addition to droplet evaporation lifetimes, the surface temperature (Figure S12), transient HoV, and total oxygenate concentration profiles for gasoline and the blends were obtained from the model (Figure 4). In comparison to gasoline, the transient HoV is significantly higher for both ethanol-containing blends and dual-alcohol blends. The reduction in HoV occurs in two steps for dual-alcohol blends while it happens once with a high slope for ethanol blends. This phenomenon makes the difference in the overall transient HoV between dual-alcohol and ethanol blends smaller than what expected from the HoV of pure alcohols. The HoV of ethanol blends and the dual counterparts are very close at early stages of evaporation until the complete evaporation of ethanol in the dual-alcohol blends where the first drop in HoV happens for dual-alcohol blends. Subsequently, the second drop happens when the higher alcohol is also evaporated completely. After depletion of oxygenates, the HoV of all blends converge with that of gasoline.

Regardless of total alcohol concentration, the dual-alcohol blends had longer droplet evaporation times compared to gasoline because of the higher HoV and larger initial droplet sizes (Figure 5). This difference is more accentuated for blends with higher blending ratios (17.1 and 8.4% increase relative to gasoline for EB40 and EH40, respectively). The dual-alcohol blends containing iso-butanol experienced slower evaporation than those with 3M3P due to the higher overall transient HoV. The only oxygenated blend that exhibited shorter evaporation time than the gasoline is E10, which can be attributed to the high vapor pressure of this blend. In the case of E20 and E40, the reduced RVP, increased HoV, and increase in droplet size compared to E10 lead to longer evaporation times relative to gasoline. The blends containing only ethanol were predicted to have ~14% shorter evaporation time on average compared to the corresponding dual-alcohol blends because of their higher volatility, regardless of slightly higher overall transient HoV. The exception is E40, which has a longer evaporation time than EH40 because the difference in HoV between E40 and EH40 is high enough to overcome the

differences in volatility. Interestingly, this is not the case with EB40 because iso-butanol has a higher HoV than 3M3P. These results indicate that once the multiple changes in properties responsible for droplet atomization and vaporization have been considered, fuels containing alcohol(s) may possess slower in-cylinder evaporation behaviors and thus could be more prone to form inhomogeneous charges that could contribute to PM emissions under heavy load or cold start. The particulate matter index (PMI) is one of the most utilized relationships to describe a fuel's tendency to form PM [33,46,47]. The PMI is a mass fraction weighted calculation which incorporates the double bond equivalent (DBE), a crude measure of chemical sooting, and the vapor pressure at 443 K (VP (443K)) to describe the evaporation tendency of for each component which makes up the complex fuel:

$$PMI = \sum_{i=1}^{n} \left[\frac{(DBE_i + 1)}{VP(443K)_i} \times Wt_i \right] \quad \text{Eq. 2}$$

Conceptually the PMI is the weighted sum of each component's chemical tendency to form soot divided by a measure of its tendency to evaporate and mix with air. Despite including a relationship between evaporation and PM emissions, the correlation does not account for non-ideal mixture vaporization behaviors (i.e., azeotropes) and does not capture evaporative cooling effects which can be important for high alcohol containing fuels. The PMI actually suggests that blending additional ethanol into a gasoline would reduce PM emissions as ethanol has a double bond equivalent of zero and a relatively high vapor pressure at 443 K, however, a number of studies have actually seen an opposite trends and poor correlations with PMI and measured PM with high alcohol containing fuels warranting the need for an improved predictive correlation to account for the vaporization properties unique to low alcohols and other oxygenated fuels [48–51].

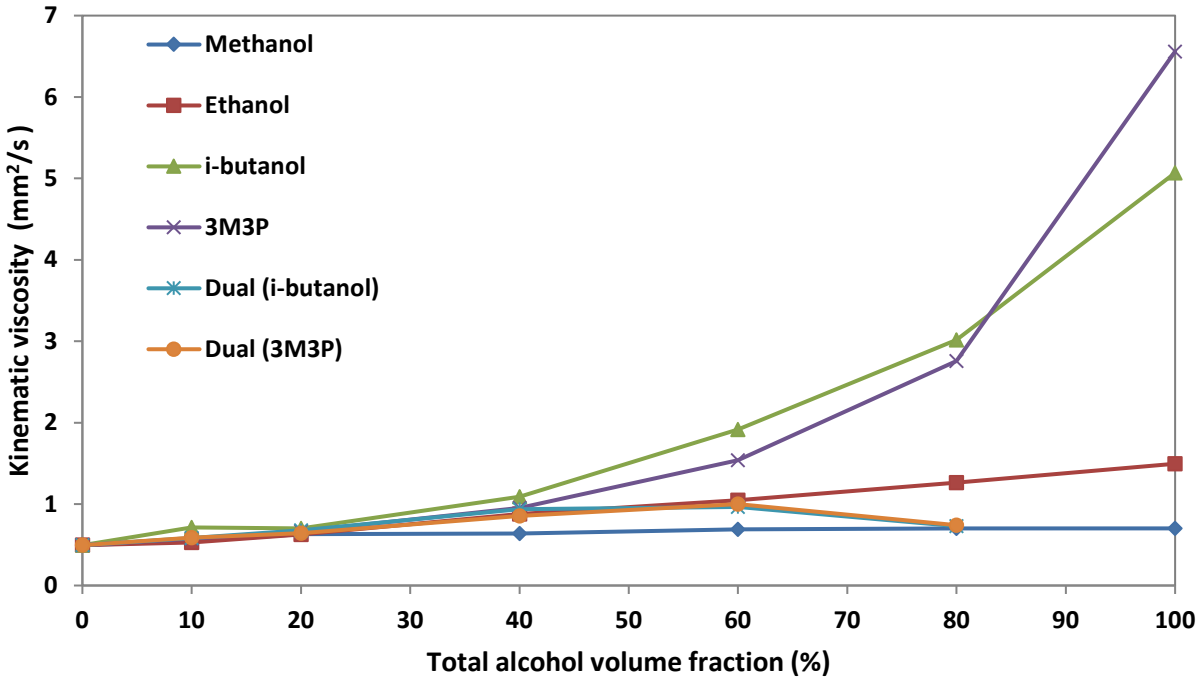

Figure 3. Kinematic viscosity at 20 °C as a function of total alcohol volume fraction. Points are the average of triplicate measurements. The average standard error for all data points is 0.2 mm^2/s.

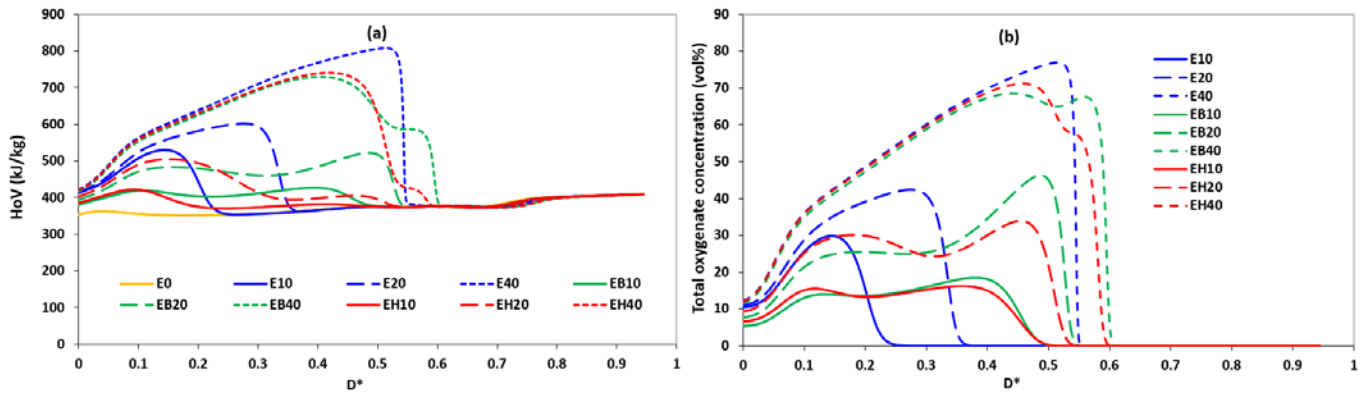

Figure 4 (a) HoV (b) Total oxygenate concentration profiles of gasoline and blend obtained from the droplet evaporation model as a function of dimensionless D^* at 1 atm and 323 K. (D_0= 25 μm). D^*=1-D/D_0. E: ethanol. B: iso-butanol. H: 3-methyl-3-pentanol

Table 5. Physical properties and corresponding droplet sizes obtained from Elkotb model [43] for test fuels. [a] Predicted by the DIPPR databases [39].

Fuel	ρ (g/cm^3)	Surface tension [a] (N/m)	v (mm^2/s)	Initial droplet size (μm)
Gasoline	0.74	0.0228	0.50	25.00
E10	0.74	0.0227	0.53	25.71
EB10	0.75	0.0228	0.58	26.91
EH10	0.75	0.0228	0.59	27.12
E20	0.75	0.0227	0.62	27.52
EB20	0.75	0.0227	0.68	28.56
EH20	0.75	0.0228	0.64	27.94
E40	0.77	0.0225	0.88	31.96
EB40	0.77	0.0226	0.94	32.80
EH40	0.76	0.0226	0.85	31.27

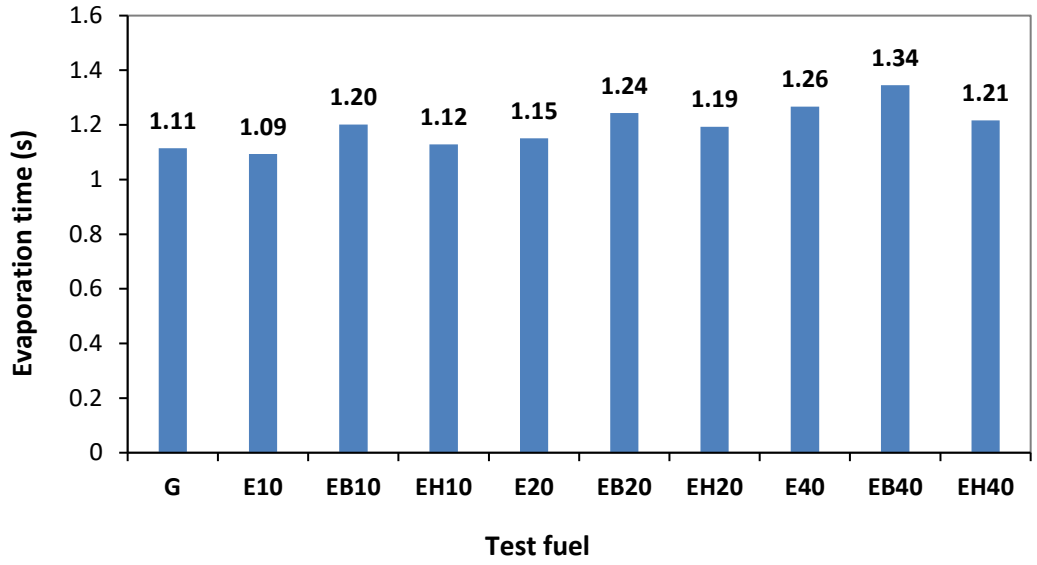

Figure 5. Droplet evaporation time for gasoline and alcohol blends obtained from the droplet evaporation model for a constant ambient pressure and temperature of 1 atm and 323 K.

3.2. Water tolerance

Gasoline and water are immiscible; however, when an alcohol is blended into gasoline, some water can also dissolve [22]. If the water tolerance of a fuel is sufficiently high to absorb the water in contact with the fuel at a given ambient temperature, no secondary corrosive phase forms. Among blends containing single alcohols, ethanol blends exhibited the highest water tolerance followed by iso-butanol, methanol, and 3M3P at 10 °C (Figure 6). Although methanol is the most polar alcohol, the results showed a very low water tolerance for the blends containing methanol. This behavior can be explained by the high hydrophilicity of methanol such that it absorbs water that is in contact with the fuel. Ethanol is more hygroscopic than the higher alcohols but not as hydrophilic as methanol, which explains why the ethanol blends had the best water tolerance behavior. Of the higher alcohols, iso-butanol had relatively good water

tolerance, especially at moderate to high blending ratios, while 3M3P had the lowest, even at high blending ratios, due to its lower polarity and longer hydrocarbon chain.

In case of the dual-alcohol blends, the concentration of the higher alcohols and total alcohol fraction were not high enough at the 10 vol% blending ratio to significantly improve the water tolerance of the gasoline. Among the 20 vol% blends, EH20 performed approximately as well as E20, while EB20 exhibited negligible water tolerance. This can be attributed to the higher concentration of ethanol in EH20 (11.5% in EH20 vs. 8.9% in EB20) as well as the lower polarity, and longer hydrocarbon chain of 3M3P. Interestingly, at blending ratios of 40 vol%, the water tolerance of both dual-alcohol blends exceeded that of the ethanol blends owing to the influence of the higher alcohols. At 60 vol%, the dual-alcohol blends significantly improved the water tolerance compared to M60 (p-value = 0.0009). Although the concentration ratio of the higher alcohols relative to the lower alcohol is very low in the 80 vol% blends, the dual-alcohol blends still had 15.3% higher water tolerance than M80.

A decrease of temperature from +10 to -10 °C led to an average decrease of 0.34 vol% in the water tolerance, suggesting that diurnal and seasonal temperature variation may influence stability. It is worth noting that the solubility of water in alcohol-gasoline blends also depends on other parameters, including humidity and fuel composition (both gasoline and alcohol) [42]. Fuels containing higher fractions of aromatics and olefins are more miscible with water due to the pi-bond in their structures [14].

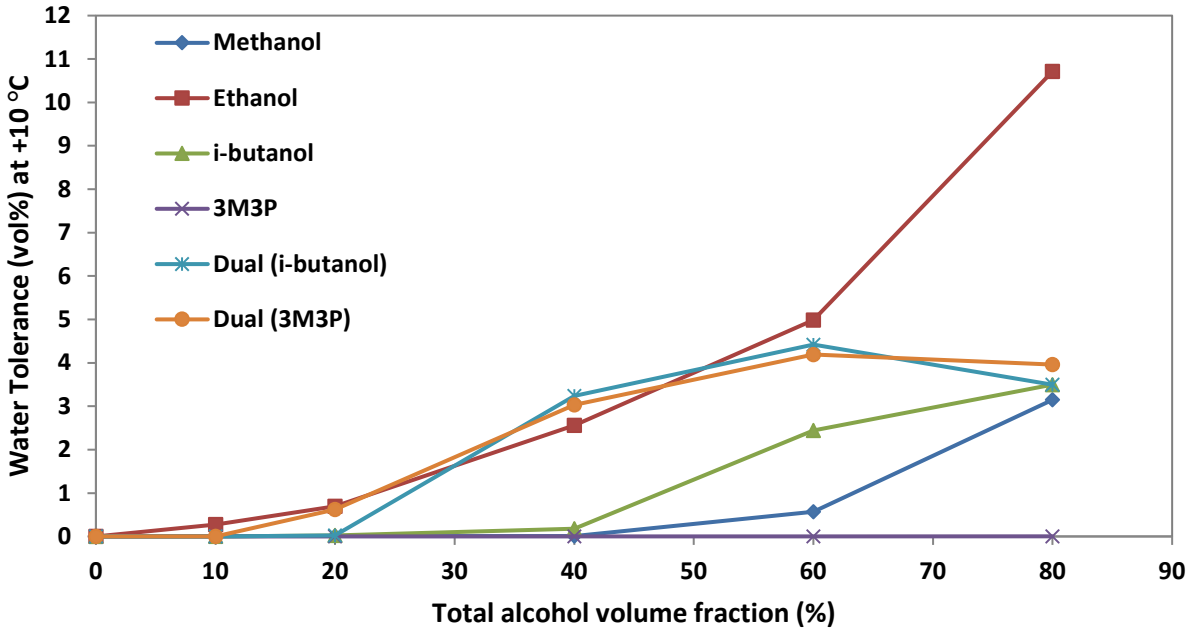

Figure 6. Water tolerance at +10 °C plotted versus total alcohol volume fraction. Points are the average of triplicate measurements. The average standard error for all data points is 0.002 vol%.

3.3. Lower heating value

Figure 7 depicts the measured LHV for the alcohol-gasoline blends as a function of the alcohol blending ratio. An approximately linear trend of decreasing LHV with decreasing carbon number can be observed for the alcohols investigated in this study due to the increase in oxygen content, with the lowest reduction in LHV from that of the gasoline observed for the 3M3P blends followed by iso-butanol, ethanol, and methanol. Applying the dual-alcohol approach did not increase the LHV of the blends notably, especially at high blending ratios. Up to 40 vol%, the LHVs of dual-alcohol blends were only an average of 0.9% higher than the ethanol blends because ethanol was the dominant alcohol component in dual-alcohol blends. At blending ratios higher than 40%, ethanol was replaced by methanol in the dual-alcohol blends and the LHV of

the dual-alcohol blends dropped dramatically. Although the lower LHV combined with higher stoichiometric air-fuel ratio of these alcohols compared to gasoline may adversely impact the fuel economy, the excellent anti-knock characteristics of these alcohols as well as their potential for charge cooling may allow the engine to operate at higher compression ratios and maximum pressures, which would increase the power output notably. Thus, considering the higher HoV, more complete combustion, and higher octane value of these alcohols, it may be possible to obtain even better BSFC using these blends.

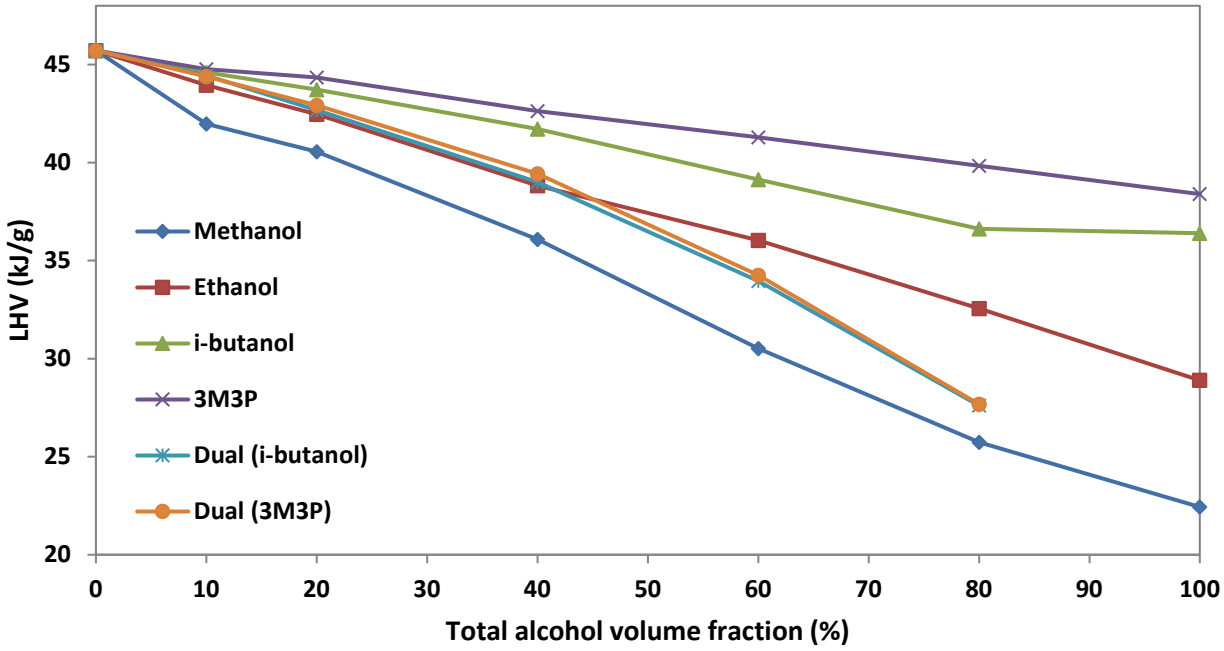

Figure 7. LHV as a function of total alcohol volume fraction for the tested blends. Points are the average of triplicate measurements. The average standard error for all data points is 0.37 kJ/g.

Conclusions

Regardless of total alcohol concentration, dual-alcohol blends could be designed to have RVP

values very close to that of gasoline. Therefore, using higher alcohols such as iso-butanol and 3-methyl-3-pentanol as components in blends of gasoline with lower alcohols appears to be a viable option to mitigate limitations associated with both high and low volatilities of gasoline blends containing a single alcohol. Results showed that it may be advantageous to use dual-alcohol blends containing up to 40 vol% as they minimize the limitations of single-alcohol blends, particularly those stemming from high or low volatility. The dual-alcohol blends exhibited satisfactory properties (volatility, kinematic viscosity, and water tolerance) for use in existing spark ignition engines. The dual-alcohol approach has potential to increase the portion of biofuel in the current gasoline system with no or only minor changes to current SI engine architectures and fuel delivery infrastructure. To build on these promising characterization results for dual-alcohol blends, future research should include material compatibility evaluation, engine and ignition quality tests, flame studies, and spray soot characteristics tests for light- and medium-duty SI engines.

Acknowledgments

This work was authored in part by Alliance for Sustainable Energy, LLC, the manager and operator of the National Renewable Energy Laboratory for the U.S. Department of Energy (DOE) under Contract No. DE-AC36-08GO28308. Funding provided by the Bioenergy Technology Office. The views expressed in the article do not necessarily represent the views of the DOE or the U.S. Government. The U.S. Government retains and the publisher, by accepting the article for publication, acknowledges that the U.S. Government retains a nonexclusive, paid-up, irrevocable, worldwide license to publish or reproduce the published form of this work, or allow others to do so, for U.S. Government purposes. This research was conducted as part of the Co-Optimization of Fuels & Engines (Co-Optima) project sponsored by the U.S. Department of Energy (DOE) Office of Energy Efficiency and Renewable Energy (EERE), Bioenergy

Technologies and Vehicle Technologies Offices. The authors also acknowledge funding from the US National Science Foundation (Grant No. DGE-0801707), and we thank Jake Martinson for his assistance with database completion.

References

[1] Elfasakhany A, Mahrous AF. Performance and emissions assessment of n-butanol–methanol–gasoline blends as a fuel in spark-ignition engines. Alexandria Eng J 2016. doi:10.1016/j.aej.2016.05.016.

[2] Rastegary J, Shirazi SA, Fernandez T, Ghassemi A. Water Resources for Algae-Based Biofuels. J Contemp Water Res Educ n.d.;151:117–22. doi:10.1111/j.1936-704X.2013.03157.

[3] Pumphrey JA, Brand JI, Scheller WA. Vapour pressure measurements and predictions for alcohol-gasoline blends. Fuel 2000. doi:10.1016/S0016-2361(99)00284-7.

[4] Regulation to mitigate the misfueling of vehicles and engines with gasoline containing greater than ten volume percent ethanol and modifications to the reformulated and conventional gasoline programs. Fed Regist 2011.

[5] Bergthorson JM, Thomson MJ. A review of the combustion and emissions properties of advanced transportation biofuels and their impact on existing and future engines. Renew Sustain Energy Rev 2015. doi:10.1016/j.rser.2014.10.034.

[6] Masum BM, Masjuki HH, Kalam MA, Rizwanul Fattah IM, M Palash S, Abedin MJ. Effect of ethanol-gasoline blend on NOx emission in SI engine. Renew Sustain Energy Rev 2013. doi:10.1016/j.rser.2013.03.046.

[7] Surisetty VR, Dalai AK, Kozinski J. Alcohols as alternative fuels: An overview. Appl Catal A Gen 2011. doi:10.1016/j.apcata.2011.07.021.

[8] Wallner T, Ickes A, Lawyer K. Analytical assessment of C2-C8 alcohols as spark-ignition

engine fuels. Lect. Notes Electr. Eng., 2013. doi:10.1007/978-3-642-33777-2_2.

[9] Sayin C. Engine performance and exhaust gas emissions of methanol and ethanol-diesel blends. Fuel 2010. doi:10.1016/j.fuel.2010.02.017.

[10] Koç M, Sekmen Y, Topgül T, Yücesu HS. The effects of ethanol-unleaded gasoline blends on engine performance and exhaust emissions in a spark-ignition engine. Renew Energy 2009. doi:10.1016/j.renene.2009.01.018.

[11] Balki MK, Sayin C, Canakci M. The effect of different alcohol fuels on the performance, emission and combustion characteristics of a gasoline engine. Fuel 2014. doi:10.1016/j.fuel.2012.09.020.

[12] Karavalakis G, Short D, Vu D, Russell RL, Asa-Awuku A, Jung H, et al. The impact of ethanol and iso-butanol blends on gaseous and particulate emissions from two passenger cars equipped with spray-guided and wall-guided direct injection SI (spark ignition) engines. Energy 2015. doi:10.1016/j.energy.2015.01.023.

[13] Masum BM, Kalam MA, Masjuki HH, Palash SM, Fattah IMR. Performance and emission analysis of a multi cylinder gasoline engine operating at different alcohol-gasoline blends. RSC Adv 2014. doi:10.1039/c4ra04580g.

[14] Mužíková Z, Pospíšil M, Šebor G. Volatility and phase stability of petrol blends with ethanol. Fuel 2009. doi:10.1016/j.fuel.2009.02.003.

[15] Shirazi SA, Abdollahipoor B, Martinson J, Reardon KF, Windom BC. Physiochemical Property Characterization of Hydrous and Anhydrous Ethanol Blended Gasoline. Ind Eng Chem Res 2018;57:11239–45. doi:10.1021/acs.iecr.8b01711.

[16] Lawyer K, Ickes A, Wallner T, Ertl D, Williamson R, Miers S, et al. Blend Ratio Optimization of Fuels Containing Gasoline Blendstock, Ethanol, and Higher Alcohols (C3-C6): Part II - Blend Properties and Target Value Sensitivity. SAE 2013 World Congr. Exhib., SAE International; 2013. doi:https://doi.org/10.4271/2013-01-1126.

[17] Thewes M, Muther M, Brassat A, Pischinger S, Sehr A. Analysis of the Effect of Bio-Fuels

on the Combustion in a Downsized DI SI Engine. SAE Int J Fuels Lubr 2011. doi:10.4271/2011-01-1991.

[18] Abdollahipoor B, Shirazi SA, Reardon KF, Windom BC. Near-azeotropic volatility behavior of hydrous and anhydrous ethanol gasoline mixtures and impact on droplet evaporation dynamics. Fuel Process Technol 2018;181:166–74. doi:https://doi.org/10.1016/j.fuproc.2018.09.019.

[19] Dahmen M, Marquardt W. Model-Based Design of Tailor-Made Biofuels. Energy and Fuels 2016. doi:10.1021/acs.energyfuels.5b02674.

[20] Fatouraie M, Wooldridge MS, Petersen BR, Wooldridge ST. Effects of Ethanol on In-Cylinder and Exhaust Gas Particulate Emissions of a Gasoline Direct Injection Spark Ignition Engine. Energy & Fuels 2015;29:3399–412. doi:10.1021/ef502758y.

[21] Ratcliff MA, Burton J, Sindler P, Christensen E, Fouts L, Chupka GM, et al. Knock Resistance and Fine Particle Emissions for Several Biomass-Derived Oxygenates in a Direct-Injection Spark-Ignition Engine. SAE Int J Fuels Lubr 2016. doi:10.4271/2016-01-0705.

[22] Christensen E, Yanowitz J, Ratcliff M, McCormick RL. Renewable oxygenate blending effects on gasoline properties. Energy and Fuels 2011. doi:10.1021/ef2010089.

[23] Yüksel F, Yüksel B. The use of ethanol-gasoline blend as a fuel in an SI engine. Renew Energy 2004. doi:10.1016/j.renene.2003.11.012.

[24] Muzikova Z, Siska J, Pospisil M, Sebor G. Phase Stability of Butanol-Gasoline Blends. vol. 107. 2013.

[25] Gautam M, Martin DW, Carder D. Emissions characteristics of higher alcohol/gasoline blends. Proc Inst Mech Eng Part A J Power Energy 2000. doi:10.1243/0957650001538263.

[26] Andersen VF, Anderson JE, Wallington TJ, Mueller SA, Nielsen OJ. Vapor pressures of alcohol-gasoline blends. Energy and Fuels, 2010. doi:10.1021/ef100254w.

[27] Siwale L, Kristóf L, Bereczky A, Mbarawa M, Kolesnikov A. Performance, combustion and emission characteristics of n-butanol additive in methanol-gasoline blend fired in a naturally-aspirated spark ignition engine. Fuel Process Technol 2014. doi:10.1016/j.fuproc.2013.10.007.

[28] Ratcliff MA, Luecke J, Williams A, Christensen E, Yanowitz J, Reek A, et al. Impact of Higher Alcohols Blended in Gasoline on Light-Duty Vehicle Exhaust Emissions. Environ Sci Technol 2013;47:13865–72. doi:10.1021/es402793p.

[29] Shirazi SA, Foust TD, Reardon KF. 2018. Development and Application of a Fuel Property Database for Mono-Alcohols as Fuel Blend Components for Spark Ignition Engines. Submitted. n.d.

[30] ASTM D5191-15 Standard Test Method for Vapor Pressure of Petroleum Products (Mini Method), West Conshohocken, PA, 2015, doi:10.1520/D5191-15 n.d.

[31] ASTM D5188-16 Standard Test Method for Vapor-Liquid Ratio Temperature Determination of Fuels (Evacuated Chamber and Piston Based Method), West Conshohocken, PA, 2016, doi:10.1520/D5188-16 n.d.

[32] ASTM D240-17 Standard Test Method for Heat of Combustion of Liquid Hydrocarbon Fuels by Bomb Calorimeter, West Conshohocken, PA, 2017, doi:10.1520/D0240-17 n.d.

[33] Aikawa K, Sakurai T, Jetter JJ. Development of a Predictive Model for Gasoline Vehicle Particulate Matter Emissions. SAE Int J Fuels Lubr 2010;3:610–22. doi:https://doi.org/10.4271/2010-01-2115.

[34] ASTM D6729-14 Standard Test Method for Determination of Individual Components in Spark Ignition Engine Fuels by 100 Metre Capillary High Resolution Gas Chromatography, West Conshohocken, PA, 2014, doi:10.1520/D6729-14 n.d.

[35] Burke SC, Ratcliff M, McCormick R, Rhoads R, Windom B. Distillation-based Droplet Modeling of Non-Ideal Oxygenated Gasoline Blends: Investigating the Role of Droplet Evaporation on PM Emissions. SAE Int J Fuels Lubr 2017. doi:10.4271/2017-01-0581.

[36] Burke S, Rhoads R, Ratcliff M, McCormick R, Windom B. Measured and Predicted Vapor Liquid Equilibrium of Ethanol-Gasoline Fuels with Insight on the Influence of Azeotrope Interactions on Aromatic Species Enrichment and Particulate Matter Formation in Spark Ignition Engines. WCX World Congr. Exp., SAE International; 2018. doi:https://doi.org/10.4271/2018-01-0361.

[37] Backhaus J. Design methodology of bio-derived gasoline fuels. 2013., 2013.

[38] Chupka GM, Christensen E, Fouts L, Alleman TL, Ratcliff MA, McCormick RL. Heat of Vaporization Measurements for Ethanol Blends Up To 50 Volume Percent in Several Hydrocarbon Blendstocks and Implications for Knock in SI Engines. SAE Int J Fuels Lubr 2015. doi:10.4271/2015-01-0763.

[39] by AIChE DI for PPS, AIChE DI for PPS by. DIPPR Project 801 - Full Version. 2005.

[40] Motor Gasolines Technical Review. Chevron n.d. https://www.chevron.com/-/media/chevron/operations/documents/motor-gas-tech-review.pdf.

[41] ASTM D86-17 Standard Test Method for Distillation of Petroleum Products and Liquid Fuels at Atmospheric Pressure, ASTM International, West Conshohocken, PA, 2017, doi:10.1520/D0086-17 n.d.

[42] Lapuerta M, García-Contreras R, Campos-Fernández J, Dorado MP. Stability, lubricity, viscosity, and cold-flow properties of alcohol-diesel blends. Energy and Fuels 2010. doi:10.1021/ef100498u.

[43] Elkotb MM. Fuel atomization for spray modelling. Prog Energy Combust Sci 1982. doi:10.1016/0360-1285(82)90009-0.

[44] Dos Santos F, Le Moyne L. Spray Atomization Models in Engine Applications, from Correlations to Direct Numerical Simulations. vol. 66. 2011. doi:10.2516/ogst/2011116.

[45] Stach T, Schlerfer J, Vorbach M. New Generation Multi-hole Fuel Injector for Direct-Injection SI Engines - Optimization of Spray Characteristics by Means of Adapted Injector Layout and Multiple Injection. SAE World Congr. Exhib., SAE International; 2007.

doi:https://doi.org/10.4271/2007-01-1404.

[46] Aikawa K, Jetter JJ. Impact of gasoline composition on particulate matter emissions from a direct-injection gasoline engine: Applicability of the particulate matter index. Int J Engine Res 2013;15:298–306. doi:10.1177/1468087413481216.

[47] Ben Amara A, Tahtouh T, Ubrich E, Starck L, Moriya H, IIda Y, et al. Critical Analysis of PM Index and Other Fuel Indices: Impact of Gasoline Fuel Volatility and Chemical Composition. Int. Powertrains, Fuels Lubr. Meet., SAE International; 2018. doi:https://doi.org/10.4271/2018-01-1741.

[48] Butler AD, Sobotowski RA, Hoffman GJ, Machiele P. Influence of Fuel PM Index and Ethanol Content on Particulate Emissions from Light-Duty Gasoline Vehicles. SAE 2015 World Congr. Exhib., SAE International; 2015. doi:https://doi.org/10.4271/2015-01-1072.

[49] Chen Y, Zhang Y, Cheng WK. Effects of Ethanol Evaporative Cooling on Particulate Number Emissions in GDI Engines. WCX World Congr. Exp., SAE International; 2018. doi:https://doi.org/10.4271/2018-01-0360.

[50] Sobotowski RA, Butler AD, Guerra Z. A Pilot Study of Fuel Impacts on PM Emissions from Light-Duty Gasoline Vehicles 2015. doi:https://doi.org/10.4271/2015-01-9071.

[51] Ratcliff MA, Windom BC, Fioroni GM, John PS, Burke S, Burton J, Christensen ED, Sindler P, McCormick RL. Impact of Ethanol Blending into Gasoline on Aromatic Compound Evaporation and Particle Emissions from a Gasoline Direct Injection Engine. Submitted.